Kinetics of Contraction of a Stiff Chain

Fabio Ganazzoli,* Roberto La Ferla, and Giuseppe Allegra

Dipartimento di Chimica, Politecnico di Milano, via L. Mancinelli 7, 20131 Milano, Italy

Received December 20, 1994; Revised Manuscript Received April 29, 1995[⊗]

ABSTRACT: The contraction kinetics of a moderately stiff chain upon sudden undercooling below the Θ temperature is investigated, adopting a freely-rotating chain model subject to intramolecular medium- and long-range interactions. The temperature-dependent two-body interactions, which vanish at $T = \Theta$, provide the driving force to collapse. The kinetic equation, derived from the appropriate nonequilibrium Langevin equation, yields the time rate of change of the contraction ratios of the Rouse−Zimm normal modes in terms of the current free-energy gradient and of the instantaneous relaxation times. For a large enough undercooling $\tau = (T - \Theta)/T$, the kinetics proceeds in two contraction steps separated by a time interval denoted as the induction time, wherein the chain size and especially the free energy remain almost constant. During the induction time, the normal modes slowly adjust to one another in a strongly cooperative process. Eventually, at a well-defined time the final contraction step takes place very quickly, leading to a relatively compact globule. From our calculations with up to 40 repeat units, the induction time scales as $N^2((\tau - \tau^*)/\tau^*)^{-1.40}$, τ^* being the critical undercooling to reach a globular state at equilibrium. Thus, the induction time may be very large for a large-molecular-weight polymer. Conversely, no induction time is found for the opposite process, i.e., the swelling of the collapsed globule to the unperturbed state. Possible connections with protein folding kinetics are briefly pointed out. The specificity of the folding behavior of each protein may be tested against the present results, although, strictly speaking, these apply only to an undifferentiated linear polymer.

Introduction

Much work has already been done on the thermodynamics of the single-chain collapse in poor solvent, both experimentally[1−3] and theoretically (see, e.g., ref 4 and references therein), as well as through computer experiments.[5] Conversely, only very few results[6,7] and some heuristic arguments have been published on the contraction kinetics to the collapsed globular state.[8,9] On the other hand, this problem is of high relevance in itself as well as a key to understand, and possibly predict, protein folding kinetics. Actually, in this paper we shall only be concerned with the kinetics of contraction of a stiff polymer consisting of identical repeat units, thus ignoring the specificity of each protein molecule as dictated by its amino acid sequence. Accordingly, from the protein viewpoint we shall deal with the early steps of chain collapse, leading to a relatively compact globule that misses a stereochemically defined organization (a sort of "molten globule"[10] that lacks also the local details of the secondary structure). Therefore, our model is still in the realm of statistics and its contraction kinetics may be tackled with average equations of motions such as the Langevin equation. By the present investigation we wish to predict the average behavior to be expected *by the very nature of a linear macromolecule*; from this viewpoint, any departures from our predictions which might be observed in a given protein should be considered as a manifestation of its specificity *in comparison with an undifferentiated polymer having the same average stiffness*.

In the present paper we report our results on the contraction kinetics of a freely-rotating chain as the simplest model of a stiff polymer. This chain, devoid of any intramolecular interaction, is denoted as the phantom chain and represents our reference state. The stiffness parameter is $g = -\cos\vartheta$, where ϑ is the angle formed by successive bond vectors connecting adjacent beads. The latter are the centers where the friction with the solvent and the intramolecular interactions are assumed to be concentrated. The beads will be denoted as "atoms" for simplicity, although representing in a coarse-grained description a relatively large number of monomers (of the order of 10, e.g.).

The intramolecular interactions considered in the present paper are the classical long-range two- and three-body interactions, taken as proportional to the corresponding probability densities of contact, and the medium-range two-body screened interactions, arising from the intrinsic thickness of the chain.[4] These are residual repulsions surviving even in the Θ state and are essentially temperature-independent, like the three-body repulsions. On the other hand, the long-range two-body interactions depend strongly on temperature, changing sign across Θ: in particular, at $T < \Theta$ they lead to chain contraction. It should be added that chain connectivity is explicitly accounted for within the three-body interactions. A further term is present in the chain free energy, namely the elastic contribution arising from the configurational entropy and opposing any departure from the phantom-chain conformation.

We shall consider chain contraction induced by the poor quality of the solvent through a sudden jump of temperature below Θ, assuming that the undercooling $\Delta T = \Theta - T$ is much smaller than Θ itself, so that the chain stiffness does not change. In a real polymer, this means that the local conformational properties, such as the population of *trans* and *gauche* states, dictating the chain stiffness, do not vary appreciably. The opposite case was specifically addressed in a recent computer simulation of the equilibrium chain collapse.[5]

The equilibrium and the dynamical description of the chain are carried out in terms of the familiar Rouse−Zimm normal modes. The Gaussian approximation will be adopted throughout, both for the normal mode amplitudes and for the interatomic distances. This approximation was theoretically substantiated for flexible chains in the globular state[11] and is adopted here throughout the range $T \leq \Theta$, although being somewhat inaccurate for very stiff chains.[12] This inaccuracy, however, is not a dramatic limitation in our case, since

[⊗] Abstract published in *Advance ACS Abstracts,* June 1, 1995.

0024-9297/95/2228-5285$09.00/0

the stiffness parameter we use is far from the rigid-rod limit $g = 1$ (see later). On the other hand, this approximation allows the chain entropic loss upon contraction to be easily obtained from the contraction ratio of the normal mode amplitudes (see the ensuing elastic free-energy term $\mathcal{A}_{el}$). The assumption of a generalized Gaussian distribution of the interatomic distances (which has nothing to do with the bead-and-spring Gaussian chain) is invoked twice: first in the two- and the three-body interaction free energy through the expression of the corresponding probability densities of contact and then in the preaveraged hydrodynamic interaction through the calculation of the reciprocal interatomic distances. Although the errors entailed by the Gaussian approximation should not be so serious as to invalidate the main conclusions, they are difficult to assess rigorously.

Mathematical Procedure

1. Phantom Chain. We consider a freely-rotating chain formed by $N + 1$ atoms and characterized by a stiffness parameter $g = -\cos\vartheta$, ϑ being the angle formed by adjacent bond vectors of length l. In the absence of intramolecular interactions, the average scalar product between any two bond vectors is given by

$$\langle \mathbf{l}_i \mathbf{l}_j \rangle / l^2 = g^{|i-j|} \tag{1}$$

whence the mean-square interatomic distances are exactly given by

$$\langle r_{ij}^2 \rangle_{ph} = l^2 |i-j| \left\{ \frac{1+g}{1-g} - \frac{2g(1-g^{|i-j|})}{|i-j|(1-g)^2} \right\} \tag{1'}$$

the ph subscript denoting the phantom state.

The equilibrium dynamics of this chain model was already studied by Perico *et al.*[13] following the approach of Zimm[14] and of Bixon and Zwanzig.[15] The approach involves a transformation of the atomic coordinates $\mathbf{R}^T = [\mathbf{R}_0, \mathbf{R}_1, ..., \mathbf{R}_N]$ into as many normal modes $\boldsymbol{\xi}^T = [\boldsymbol{\xi}_0, \boldsymbol{\xi}_1, ..., \boldsymbol{\xi}_N]$:

$$\boldsymbol{\xi} = \mathbf{Q} \cdot \mathbf{R} \tag{2}$$

$\mathbf{Q}$ is obtained by solving the eigenvalue equation

$$\mathbf{H} \cdot \mathbf{A} \cdot \mathbf{Q} = \mathbf{Q} \cdot \boldsymbol{\Lambda} \tag{3}$$

where the elements of the diagonal matrix $\boldsymbol{\Lambda}$ provide the spectrum of the (adimensional) chain relaxation rates. The matrix $\mathbf{A}$ is given by[13,15]

$$\mathbf{A} = \frac{1-g}{1+g} \mathbf{A}_R + \frac{g}{1-g^2} \mathbf{A}_R^2 - \frac{g^2}{1-g^2} \Delta \tag{4}$$

where $\mathbf{A}_R$ is the Rouse matrix[14] and Δ a perturbation which is negligible except for very stiff (i.e., $g \to 1$) or very short chains. The matrix $\mathbf{H}$ gives the hydrodynamic interaction in the preaveraging approximation. Its elements are[13,14]

$$H_{ij} = \delta_{ij} + \zeta_r \left\langle \frac{l}{r_{ij}} \right\rangle (1 - \delta_{ij}) \tag{5}$$

where δ_{ij} is the Kronecker delta and ζ_r the reduced friction coefficient:

$$\zeta_r = \frac{\zeta}{6\pi\eta_S l} \tag{5'}$$

ζ being the atomic friction coefficient and η_S the solvent viscosity. Within the Gaussian approximation, the reciprocal averages in eq 5 are given by

$$\langle r_{ij}^{-1} \rangle = \left(\frac{6}{\pi \langle r_{ij}^2 \rangle} \right)^{1/2} \tag{6}$$

The λ_p elements of the matrix $\boldsymbol{\Lambda}$ in eq 3 are real and nondegenerate and can be ordered into a monotonically increasing succession starting from a zero value (for $p = 0$) related to the diffusion of the center of mass. The relaxation times τ_p are given by ($p \neq 0$)

$$\tau_p = (\sigma \lambda_p)^{-1} \tag{7}$$

where $\sigma = 3k_B T/\zeta l^2$, and in turn λ_p, may be written as

$$\lambda_p = \mu_p \nu_p \tag{8}$$

where μ_p and ν_p are the diagonal elements of the matrices

$$\boldsymbol{\mu} = \mathbf{Q}^T \cdot \mathbf{A} \cdot \mathbf{Q} \tag{9}$$

$$\boldsymbol{\nu} = \mathbf{Q}^{-1} \cdot \mathbf{H} \cdot (\mathbf{Q}^{-1})^T \tag{10}$$

In the free-draining approximation $\zeta_r = 0$, and $\boldsymbol{\nu}$ reduces to the unit matrix of order $(N+1) \times (N+1)$. The first element of $\boldsymbol{\mu}$, i.e., μ_0, is always equal to zero.

The Langevin equation for the pth normal mode is simply given by[16,17]

$$\frac{\partial \boldsymbol{\xi}_p}{\partial t} + \sigma \lambda_p \boldsymbol{\xi}_p = \boldsymbol{v}_p \tag{11}$$

where $\boldsymbol{v}_p$ is a random velocity.

2. Intramolecular Free Energy of the Perturbed Chain. We now consider an unperturbed freely-rotating chain subject to intramolecular interactions. At time $t = 0$ we suddenly change the solvent quality and follow the time evolution of the average chain conformation. Let us define the diagonal matrix $\boldsymbol{\alpha}^2(t)$ whose elements $\alpha_p^2(t)$ are the mean-square strain ratios at time t of the pth normal mode[18] with respect to the phantom chain. We write

$$\alpha_p^2(t) = \alpha_p^2(0) \langle [\xi_p(t)]^2 \rangle / \langle [\xi_p(0)]^2 \rangle \qquad p = 1, 2, ..., N \tag{12}$$

where the value at $t = 0$, i.e., $\alpha_p^2(0)$, is the strain ratio of the unperturbed chain with respect to the reference phantom state:

$$\alpha_p^2(0) = \langle [\xi_p(0)]^2 \rangle / \langle (\xi_p)^2 \rangle_{ph} \tag{12'}$$

This quantity will be derived later.

We now make the assumption that the eigenvector matrix $\mathbf{Q}$ stays unchanged throughout the kinetic process, thus being equal to that obtained for the phantom chain (see eqs 3–5). Conversely, both $\mathbf{A}$ and $\mathbf{H}$ change with time. However, the new $\mathbf{A}(t)$ matrix need not be evaluated explicitly; in fact, following refs 4 and 19, we may write

$$\mathbf{Q}^T \cdot \mathbf{A}(t) \cdot \mathbf{Q} = \boldsymbol{\mu} (\boldsymbol{\alpha}^2(t))^{-1} \tag{13}$$

where $\boldsymbol{\mu}$ is kept unchanged (see eqs 4 and 9) and the effect of chain deformation is embodied in $\boldsymbol{\alpha}^2(t)$. On the other hand, $\mathbf{H}(t)$ is still given by eqs 5 and 6, but with

the current $\langle r_{ij}^2(t)\rangle$ values which do change with time. In turn, these are given by[4,17]

$$\langle r_{ij}^2(t)\rangle = l^2\sum_{p=1}^{N}(Q_{ip} - Q_{jp})^2\frac{\alpha_p^2(t)}{\mu_p} \tag{14}$$

(We checked that for the phantom chain, i.e., for $\alpha_p^2(t) \equiv 1$, this equation yields the same values as eq 1.) Incidentally, from the latter expression the mean-square radius of gyration turns out to be

$$\langle S^2(t)\rangle = (N+1)^{-2}\sum\sum_{i<j}\langle r_{ij}^2(t)\rangle$$

$$= l^2N^{-1}\sum_{p=1}^{N}\frac{\alpha_p^2(t)}{\mu_p} \tag{14'}$$

whereas the hydrodynamic radius is given by

$$R_H^{-1} = \frac{1}{(N+1)\zeta_r l} + \frac{1}{(N+1)^2}\sum\sum_{i\neq j}\left\langle\frac{1}{r_{ij}}\right\rangle \tag{14''}$$

If at time $t = 0$ we suddenly change the solvent quality, the chain free energy decreases monotonically with time to a new minimum. With the phantom chain as the reference state, the free energy is written as,[4] in k_BT units

$$\mathcal{A}(t) = \mathcal{A}_{el} + \mathcal{A}_{intra} \tag{15}$$

where the elastic contribution of entropic origin is

$$\mathcal{A}_{el} = \frac{3}{2}\sum_{p=1}^{N}[\alpha_p^2(t) - 1 - \ln \alpha_p^2(t)] \tag{16}$$

whereas the intramolecular part is expressed as, in the generalized Gaussian approximation,

$$\mathcal{A}_{intra} = \mathcal{A}_2 + \mathcal{A}_{2S} + \mathcal{A}_3 \tag{17}$$

$$\mathcal{A}_2 = \tau B\sum\sum_{i<j}[\langle r_{ij}^2(t)\rangle/l^2]^{-3/2} \tag{18}$$

$$\mathcal{A}_{2S} = K\sum\sum_{i<j}[\langle r_{ij}^2(t)\rangle/l^2]^{-5/2} \tag{19}$$

$$\mathcal{A}_3 = K_1\sum\sum\sum_{i<j<h}\Psi_{ijh}(t)^{-3/2} \tag{20}$$

$$\Psi_{ijh}(t) \equiv \Psi[\langle r_{ij}^2(t)\rangle/l^2, \langle r_{ih}^2(t)\rangle/l^2, \langle r_{jh}^2(t)\rangle/l^2]$$

$$\Psi(x,y,z) = \frac{1}{2}(xy + xz + yz) - \frac{1}{4}(x^2 + y^2 + z^2) \tag{20'}$$

In the above equations, $\mathcal{A}_2$ gives the long-range two-body free energy; this is repulsive for $T > \Theta$ [hence $\tau = (T - \Theta)/T > 0$], leading therefore to good-solvent expansion, whereas it is attractive for $T < \Theta$ [i.e., $\tau = (T - \Theta)/T < 0$], corresponding to poor-solvent contraction. $\mathcal{A}_{2S}$ (for the screened interactions) and $\mathcal{A}_3$ (for the three-body interactions) give the repulsive contributions which are important only in the Θ state and in the poor-solvent regime. B, K, and K_1 are positive dimensionless constants.[4,18] $\Psi_{ijh}^{-3/2}$ is proportional to the contact probability density among atoms i, j, and h and gives rise to long-range interactions, unlike the screened interactions (note the different exponents). Only for the *phantom freely-jointed* chain does this probability density factorize into the product of the contact probability densities between the two atom pairs i,j and j,h (since then $\Psi_{ijh}(t) = l^{-4}\langle r_{ij}^2(t)\rangle\langle r_{jh}^2(t)\rangle$, see the Appendix), whereas in general this is not true. It may also be shown[4] that the requirement $\Psi_{ijh} > 0$ correctly accounts for the chain connectivity.

3. Kinetic Equation. During chain deformation, the nonstationarity of the chain free energy gives rise to an extra term in the dynamical equation. The problem was already dealt with by two of us in ref 18; from the general Langevin equation, the following kinetic equation for $\alpha_p^2(t)$ was derived:

$$\frac{d\alpha_p^2(t)}{dt} = -\frac{4}{3}\sigma\nu_p(t)\,\mu_p\alpha_p^2(t)\frac{\partial\mathcal{A}(t)}{\partial\alpha_p^2(t)} \qquad p = 1, 2, ..., N \tag{21}$$

Note that the mode with $p = 0$ is absent, being related to the center-of-mass diffusion only; it is therefore irrelevant to chain conformation. In the above equation, $\nu_p(t)$ is the pth diagonal element of matrix $\boldsymbol{\nu}(t)$ obtained from eqs 5, 6, 10, and 14 with the current values of the $\alpha_p^2(t)$'s. The free-energy gradient is written explicitly in the Appendix, eqs A-3 to A-5. In the kinetic eq 21 all the modes are coupled both through the hydrodynamic interaction terms $\nu_p(t)$ and through the free-energy derivative: in either case, the full set of the mean-square interatomic distances is required, and these are given in eq 14 by a sum over all the modes. This mode coupling suggests that the chain deformation may imply a large amount of cooperativity among the modes.

Note that upon setting $\partial\mathcal{A}/\partial\alpha_p^2 = 0$ ($p = 1, 2, ..., N$) (see eq A-3) and disregarding the time dependence, i.e., upon direct free-energy minimization, we get together with eq 14 a self-consistent set of equations yielding the equilibrium state. In this way, in particular, the strain ratios of the unperturbed state with $\tau B = 0$, that is, $\alpha_p^2(0)$ in eq 12', may be easily obtained. Alternatively, they may be obtained through the kinetic equations by setting $\tau B = 0$ in the long time limit (in practice, when both $\alpha_p^2(t)$ and $\mathcal{A}(t)$ do not change any more). We checked that the two procedures (see also the next sections) yield the same equilibrium values within the numerical accuracy for any τB. In the following, we shall append a subscript zero to indicate the actual unperturbed state of the chain with intramolecular interactions at $\tau B = 0$ (i.e., at $T = \Theta$), since this is the experimentally accessible state, unlike the phantom state.

Numerical Procedure

The kinetic differential equations were solved through simple finite differences, with an automatically calibrated and varying time step. Upon definition of a maximum time step Δt_{max}, the given computation tolerance had to be satisfied relative to the final results (i.e., the results after the time step) and not on the basis of local derivatives. Starting from the generic time value $t = n\Delta t_{max}$, we compared the results at time $t + \Delta t_{max}$ obtained with an increasing number of finite difference calculations performed with integer fractions of Δt_{max}. These fractions were computed by subsequent bisections, thereby entailing the computation of the kinetics from $n\Delta t_{max}$ to $(n + 1)\Delta t_{max}$ by 2^k finite difference schemes. If $\alpha_p^2(2^k)$ is the square strain ratio of the pth normal mode computed for this time interval using 2^k

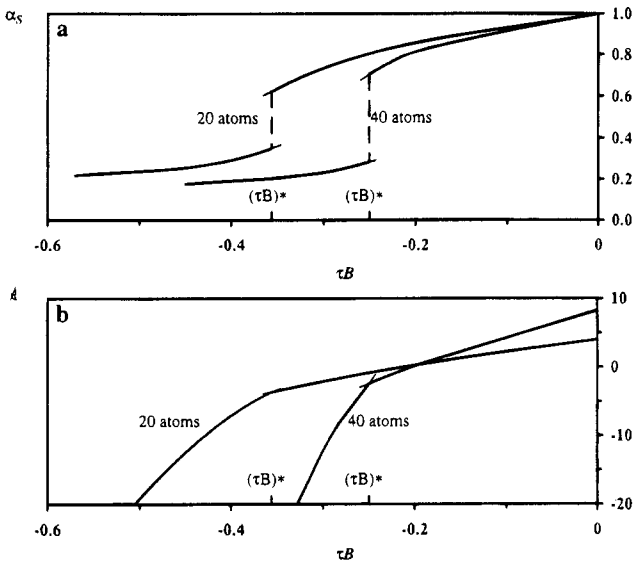

Figure 1. Equilibrium contraction ratio α_S (a) and the equilibrium excess free energy $\mathcal{A}$ in k_BT units (b) plotted as a function of the undercooling τB [$\tau = (T - \Theta)/T$] for freely-rotating chains ($g = 1/e$) of two different lengths (indicated on the curves). The thin solid curves represent metastable states. The transition coordinates $(\tau B)^*$ are indicated; in both cases the reduced variable $(\tau B)^*\sqrt{N}$ is equal to -1.59 (see text).

time steps (finite difference schemes), the convergence was deemed to be satisfactory when

$$\frac{|\alpha_p^2(2^k) - \alpha_p^2(2^{k+1})|}{\alpha_p^2(2^{k+1})} < \epsilon$$

for any mode p, wherein ϵ is the required tolerance, in the range 10^{-5} to 10^{-6}. The equilibrium results were obtained independently by a numerical iterative procedure as done previously in similar works.[18,20]

The parameters held fixed throughout the calculations were chosen as $K = 0.3$ and $K_1 = 2 \times 10^{-3}$. The latter is equal to that used to fit equilibrium results of atactic polystyrene in poor solvent,[2,21] the former was chosen as representative of a relatively "thick" polymer; in this way, the final globule state is not very compact and still includes a relatively large fraction of solvent. As for the chain stiffness parameter, it was taken as $g = 1/e$, e being the base of the natural logarithms, so that the effective bond length roughly corresponds to one persistence length. In fact, a stiff model is often described as a wormlike chain, which may be viewed as the continuous limit of the freely-rotating chain. A "bond" of the present model may then be taken to represent a persistence length of the wormlike chain in that the average cosine between two consecutive "bonds" has the same value $1/e$ as between the tangent vectors at two points along the wormlike chain if they are separated by just one persistence length. The number of atoms was chosen as equal to 10, 20, and 40, matching the number of persistence-length segments used in a previous work on globular proteins.[22]

Results and Discussion

Let us first consider the equilibrium results. At first, upon decreasing τB below the unperturbed value of zero, the freely-rotating chain contracts smoothly: its strain ratio $\alpha_S = [\langle S^2\rangle/\langle S^2\rangle_0]^{1/2}$ decreases with continuity from the unit value; see Figure 1a (note that the unperturbed value $\langle S^2\rangle_0$ is larger than the phantom chain value by a factor 1.64 due to the medium-range screened interactions and, to a lesser extent, to the long-range three-body interactions). If the number of atoms is large enough (20 or 40), at the value $(\tau B)^*$ there is a discontinuous transition to a collapsed state, which slowly contracts upon further decreasing τB. Correspondingly, the equilibrium free energy plotted as a function of τB (see Figure 1b) shows a discontinuity in its first derivative at $(\tau B)^*$ indicative of a (pseudo) first-order transition in the thermodynamic limit. In the neighborhood of $(\tau B)^*$, two minima in the free energy are present, the shallower one representing metastable states (thin solid curves in Figure 1). This means that the experimentally observable α_S is given by the weighted average of the two values, the weight factors being proportional to the corresponding Boltzmann factors $\exp(-\mathcal{A})$. Conversely, no discontinuity is observed for the shorter chain ($N = 10$), and the corresponding free-energy plot is continuous with its first derivative. The transition coordinate $(\tau B)^*$ may then be taken as the inflection point of the plot of α_S vs τB. The peculiarity of this transition was already discussed in ref 20. It should be added that using the reduced variable $\tau B\sqrt{N}$ a universal transition coordinate is found in any case, namely $(\tau B)^*\sqrt{N} \cong -1.59$. The present results indicate that the transition becomes sharper with increasing chain length for a given stiffness, in agreement with previous suggestions. Since this aspect of chain collapse has been studied in previous work (see, e.g., refs 22–24) and is not the main issue here, we shall not comment further on it.

We now turn to the kinetic aspects. Starting from the unperturbed chain, at time $t = 0$ we suddenly impose a given $\tau B < 0$ and follow the changes of chain dimensions and free energy as a function of time. Within the reduced temperature range $0 > \tau B > (\tau B)^*$, the equilibrium state is characterized by a relatively small contraction from the unperturbed state. Correspondingly, both the chain free energy and the chain size (either the mean-square radius of gyration or the hydrodynamic radius) decrease smoothly with time to the equilibrium value, corresponding to a minimum of the chain free energy. The plots of the free energy $\mathcal{A}(t)$, of $\alpha_S(t) = [\langle S^2(t)\rangle/\langle S^2\rangle_0]^{1/2}$ and of $\alpha_H(t) = R_H(t)/R_{H_0}$ are shown as a function of time (in adimensional units σt) in Figure 2 for a typical case ($N = 20$, $\tau B = -0.20$). Except for very short times, these quantities change exponentially with different characteristic times t_c somewhat shorter than the longest equilibrium relaxation time of the unperturbed chain. The differences in t_c are to be attributed to the relative weights of the various modes yielding, for example, $\langle S^2\rangle$ and $\mathcal{A}$. In particular, the radius of gyration is mostly influenced by the collective modes, whereas all the modes play about the same role in determining $\mathcal{A}$ (see for example $\mathcal{A}_{el}$ in eq 16). Therefore, it is of interest to monitor the time change of the root-mean-square contraction ratios α_p of the normal-mode amplitudes (see Figure 3; actually, here we report for consistency the ratios $\alpha_p(t)/\alpha_p(0)$ relative to the unperturbed Θ state). At short times, only the localized modes ($p \gg 1$) undergo a significant contraction because of their small relaxation times, whereas the first mode is the slowest to change because it has the largest relaxation time. On the other hand, it eventually undergoes the largest contraction at long times. Therefore, the free energy $\mathcal{A}$ attains its equilibrium value sooner than α_S since the internal modes

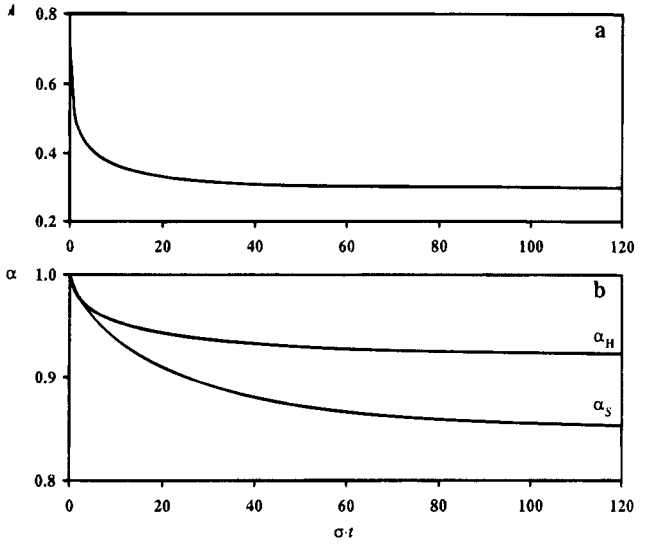

Figure 2. Excess free energy $\mathcal{A}(t)$ in k_BT units (a) and the contraction ratios $\alpha_S(t)$ and $\alpha_H(t)$ (b) at the undercooling $\tau B = -0.20$ [$>(\tau B)^*$] plotted as a function of σt for $N = 20$.

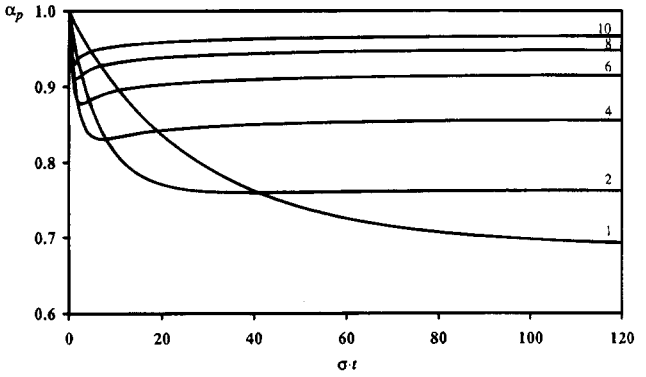

Figure 3. Contraction ratio of the root-mean-square mode amplitudes α_p relative to the unperturbed state plotted as a function of σt for the chain of Figure 2 [$\tau B = -0.20 > (\tau B)^*$, $N = 20$]. The normal-mode indices are reported on the curves.

relax quickly, whereas α_S basically follows the same contraction kinetics as the first mode. Incidentally, this result indicates that the free energy becomes virtually stationary, while the chain size is still changing appreciably.

The kinetic behavior is qualitatively similar throughout the reduced temperature range $0 > \tau B > (\tau B)^*$, the overall kinetics being accelerated, the more so the larger is $|\tau B|$. This is due to the larger gradient of the free energy which affects more strongly the collective modes, and therefore the equilibrium values of the α_p's are attained at increasingly similar times with an increasingly similar pattern.

An entirely different kinetic pattern is observed for a larger attractive potential, i.e., for $\tau B < (\tau B)^*$. Taking again $N = 20$ as an example and starting again from the unperturbed state at $t = 0$, at first the chain contracts as before: both the free energy [$\mathcal{A}(t)$ in Figure 4a] and the chain size [see $\alpha_S(t)$ and $\alpha_H(t)$ in Figure 4b,c] decrease exponentially with time (apart from very short times). Afterward, the contraction kinetics is sharply slowed down while the overall conformation is still far from equilibrium. Eventually, the right path is found and the true equilibrium, corresponding to the globular state, is reached very quickly at a rather well-defined time $(\sigma t)_{final}$ which depends on τB. The time interval wherein this slowing down is observed will be denoted as the *induction time*; its most straightforward estimate

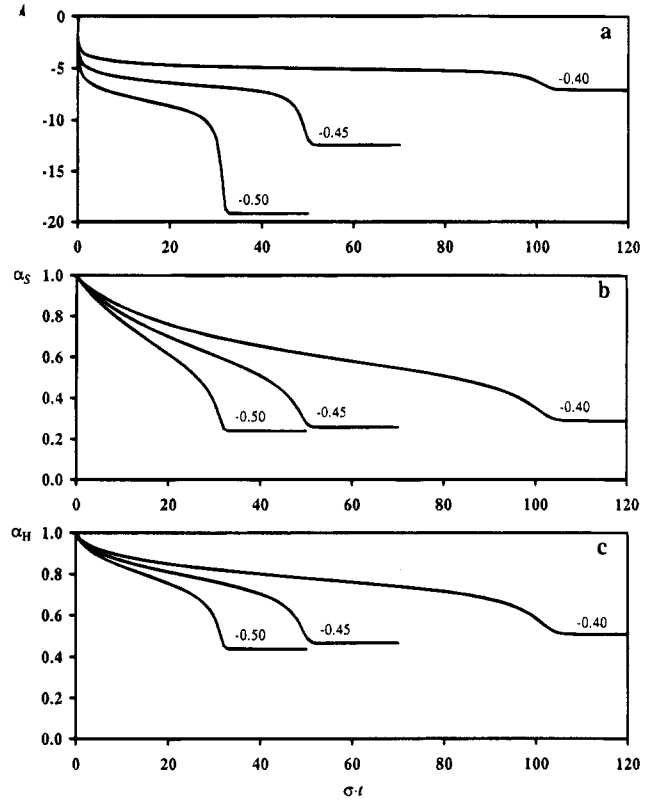

Figure 4. Excess free energy $\mathcal{A}(t)$ (a) and the contraction ratios $\alpha_S(t)$ and $\alpha_H(t)$ [(b) and (c)] plotted as a function of σt at $\tau B < (\tau B)^*$ (different τB values are reported on the curves, $N = 20$). To put the time scale into perspective, the longest relaxation time of the 20-atom unperturbed chain is $\sigma\tau_1 = 85$.

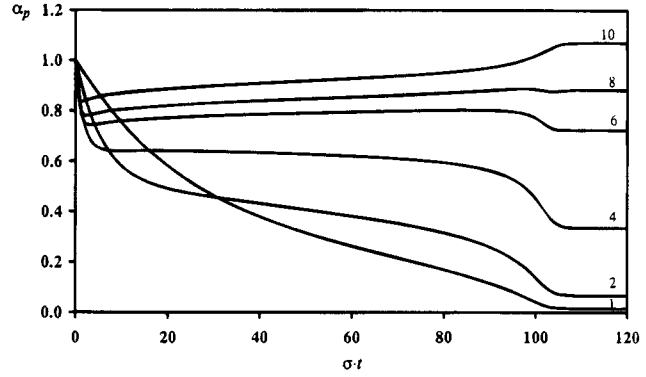

Figure 5. Contraction ratio of the root-mean-square mode amplitudes α_p relative to the unperturbed state plotted as a function of σt for the chain with $N = 20$ at $\tau B = -0.40 < (\tau B)^*$. The normal-mode indices are reported on the curves.

can be taken as $(\sigma t)_{final}$ itself, in view of the very fast final contraction.

The slowing down of the contraction rate is most evident in the free-energy plots and is due to the need of the normal-mode amplitudes to adjust to each other in a cooperatively, finely tuned way. A typical plot of some α_p's as a function of time is reported in Figure 5. The collective *internal* modes ($2 \le p \le 6$) undergo little changes at intermediate times, approaching a plateau value before the final sharp contraction, whereas the slowing down is much less evident for the first mode. Conversely, the more localized modes ($p > 8$) undergo an initial fast contraction thanks to their short relaxation times and then they slowly expand somewhat when the induction time has elapsed, eventually yielding a local swelling of the chain with a final amplitude even larger than in the unperturbed state (i.e., $\alpha_p > 1$

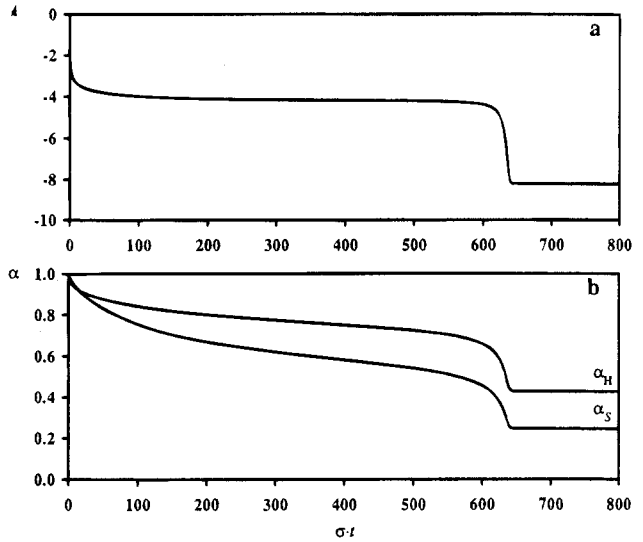

Figure 6. Excess free energy $\mathcal{A}(t)$ (a) and the contraction ratios $\alpha_S(t)$ and $\alpha_H(t)$ (b) plotted for the chain with $N = 40$ as a function of σt at $\tau B = -0.283 < (\tau B)^*$. The reduced variable $\tau B\sqrt{N} = -1.79$ corresponds to the case $\tau B = -0.40$ for $N = 20$. To put the time scale into perspective, the longest relaxation time of the 40-atom unperturbed chain is $\sigma\tau_1 = 256$.

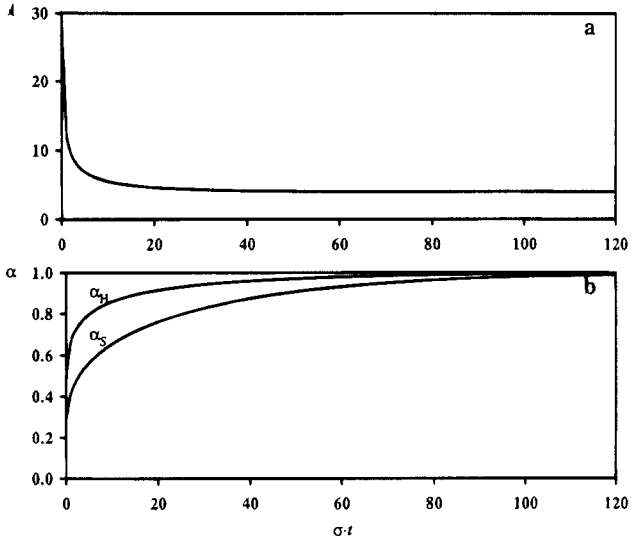

Figure 7. Excess free energy $\mathcal{A}(t)$ (a) and the contraction ratios $\alpha_S(t)$ and $\alpha_H(t)$ (b) as a function of time for $N = 20$ during the unfolding kinetics to the unperturbed state. At $\sigma t = 0$, τB is set to zero while the chain is in the globular state reached at $\tau B = -0.40$.

for $p > 8$). In this way, the chain can relieve some of the strain which otherwise it would experience at all scales. This kinetic behavior dictated by the chain cooperativity is also related to the stringent constraints imposed by the packing requirements.

It is evident from Figure 4 that the closer τB is to the transition coordinate $(\tau B)^*$, the larger is the induction time and the more pronounced the slowing down of the free energy rate of change. An inverse relationship exists between $(\sigma t)_{\text{final}}$ (our best estimate of the induction time) and $\Delta\tau B = |\tau B - (\tau B)^*|$, whereas the induction time increases strongly with N even at the same reduced variable $\tau B\sqrt{N}$ (remember that $(\tau B)^*\sqrt{N} = -1.59$ is the universal transition coordinate). In fact, Figure 6 reports $\mathcal{A}(t)$, $\alpha_S(t)$, and $\alpha_H(t)$ for a chain with 40 atoms at $\tau B = -0.283$ for a comparison with the 20-atom chain at $\tau B = -0.40$, so that in both cases we have $\tau B\sqrt{N} = -1.79$. It may be noted that the two induction times are vastly different, even with respect to the longest relaxation times in the unperturbed state ($\sigma\tau_1 = 85$ for $N = 20$ and $\sigma\tau_1 = 256$ for $N = 40$). For large enough N, our results may be expressed by the equation

$$(\sigma t)_{\text{final}} \cong CN^2\left|\frac{\tau B - (\tau B)^*}{(\tau B)^*}\right|^{-\gamma} \qquad (22)$$

where $C = 0.023 \pm 0.001$ and $\gamma = 1.40 \pm 0.01$ were determined by a least-squares fit, whereas the exponent of N was a best guess. A more accurate evaluation of γ and of the power-law dependence of N would require calculations with longer chains, which are currently outside our computer time possibilities. Some deviations from eq 22 are present for the shorter chains if τB is very close to $(\tau B)^*$: in this case, the induction time tends to infinity even faster than predicted by this equation, provided there is a discontinuity in the equilibrium plots of α_S. In any case, eq 22 implies that in a large-molecular-weight polymer $(\sigma t)_{\text{final}}$ may be much larger than the largest relaxation time of the unperturbed chain, since the latter will eventually scale with N like $N^{3/2}$. The existence of such a lengthy induction time reflects the high degree of cooperativity required by the chain at all scales to find the appropriate path to a compact, though random, structure; in turn, the cooperativity is related to the connectivity of the macromolecule and enhanced by its stiffness.

A sort of limiting case of a very long and flexible chain ($N = 5 \times 10^4$, $g = 0$) was treated by us in ref 18. In that case, the huge number of normal modes required such a large cooperativity as to make the collapse kinetics virtually frozen. Therefore, we suggested that a metastable state was possibly reached, corresponding to a local free-energy minimum. The present results actually seem to favor the hypothesis that the free-energy surface permits a decreasing path, although very flat, to equilibrium, but we cannot rule out the alternative possibility that a true (relative) free-energy minimum exists at a sufficiently large molecular weight.

An entirely different result is obtained for the unfolding kinetics, which does not show any induction time. Considering a chain that has reached the equilibrium globular state at a given τB (=−0.4 in the present case, $N = 20$), we switch back to $\tau B = 0$; i.e., we bring it back to the Θ temperature and follow the unfolding kinetics from this time onward. The corresponding time change of the free energy $\mathcal{A}(t)$ and of the strain ratios $\alpha_S(t)$ and $\alpha_H(t)$ are reported in Figure 7. The strain ratios increase exponentially to the unperturbed value (Figure 7b), while the free energy (which obviously decreases, see Figure 7a) becomes virtually stationary rather soon. This result is consistent with the lack of constraints during expansion; furthermore, the chain ends tend to lie outside the globule for entropic reasons,[11] thus making the process easier.

A two-stage collapse kinetics was observed recently by Chu *et al.*[6,7] through dynamic light scattering. A large-molecular-weight ($M_w = 8.6 \times 10^6$) and relatively monodisperse ($M_z/M_w = 1.08$) atactic polystyrene in a very diluted cyclohexane solution was quenched to 6−7 deg below Θ; the hydrodynamic radius was then monitored as a function of time. At first, the coil contracts to $\alpha_H = 0.83$[6] (or 0.71 in ref 7), then its size remains constant for some 2 h, according to ref 6, or about 6 min, according to ref 7 (one possible source of the difference should be attributed to the slightly larger undercooling in the latter case and to the possible thermal inertia of the thicker cells employed in the former case). After-

ward, a further contraction takes place to a final value[6] of $\alpha_H = 0.38$ (or 0.31 in ref 7). Some polymer aggregation takes place at the same time, involving only a few percent of the molecules. However, its contribution to the scattering could be confidently separated from that due to the single chains long before all the chains aggregate; the effect of fractionation on α_H could be taken as negligible in view of the low polydispersity. Interestingly, both contraction steps were fitted by simple exponentials of the form $R_H = A \exp(-t/t_c)$, where $t_c = 357$ s for the first stage and $t_c = 327$ s for the final stage. Thus, the second contraction step appears to be at least as fast as the first one, in qualitative agreement with our results, although the difference is hardly significant. Chu *et al.*[6,7] compared their results with the theoretical predictions of Grosberg and Kuznetsov.[9] These authors describe the chain collapse as a two-step process: the first step involves the contraction to a "crumpled globule" with an intermediate degree of compression in a relatively fast time proportional to N^2; the second step consists of a knotting process of a reptational character, thereby requiring a larger time[9] proportional to N^3. Fitting their results to these predictions, Chu *et al.* obtained a reasonable density of the globule, although the time scales do not appear to be fully consistent with the theoretical estimates.

Our results, and in particular the faster second stage of contraction, cannot be reproduced by any monomolecular kinetic scheme involving three distinct species A, B, and C, respectively, corresponding to the unperturbed coil, to the "crumpled globule" during the induction time, and to the collapsed globule. Rather, an autocatalytic second step must be invoked, accelerated by the amount of the final product, and roughly corresponding to the degree of cooperativity among the normal modes discussed above. Specifically, the kinetic features of the present approach can be modeled with a three-state irreversible reaction model, wherein at first A undergoes a simple monomolecular "crumpling" step with a kinetic constant k_1; then, the "crumpled globule" B shows either a simple monomolecular collapse with a kinetic constant k_2 or a cooperative, autocatalytic collapse to the globular state with a kinetic constant k_3 according to the following scheme

$$A \xrightarrow{k_1} B \xrightarrow{k_2} C$$

$$B + 2C \xrightarrow{k_3} 3C$$

Denoting with f_X the instantaneous fraction of the X species, the kinetic equations are

$$\left(\frac{\partial f_A}{\partial t}\right)_T = -k_1 f_A$$

$$\left(\frac{\partial f_B}{\partial t}\right)_T = k_1 f_A - k_2 f_B - k_3 f_B f_C^2$$

$$\left(\frac{\partial f_C}{\partial t}\right)_T = k_2 f_B + k_3 f_B f_C^2 \qquad (23)$$

At any given time t, $\alpha_S(t)$, $\alpha_H(t)$, and $\mathcal{A}(t)$ are obtained as the weighted average of the corresponding quantities for each of the three species, each contributing with its appropriate value. The larger is the k_3 constant, the sharper is the final collapse step at $t = (\sigma t)_{final}$, whereas the smaller is k_2, the longer is the induction time; within this time interval, only the B species is present (i.e., $f_B \cong 1$), whereas A has already disappeared and C has not yet formed in appreciable quantity. Conversely, if the autocatalyzed process is not much faster than the simple monomolecular collapse, no cooperativity is needed and the collapse kinetics does follow a simple exponential such as in Figure 2. Intermediate kinetics can be obtained by suitably changing the k_2/k_3 ratio. However, no attempt is made here to adjust the values of the kinetic constants so as to correlate them with changes in the parameters employed in the paper, since this kinetic model bears only a rough analogy to our results. In fact, our collapse kinetics is strictly monomolecular and the normal-mode description prevents any simple translation in terms of real intermediates, yielding only the time evolution of a single, average molecule. Thus, the autocatalytic process reflects only *the required cooperativity among all the normal modes*. To put it otherwise, we may say that in our picture the "catalyst" does not consist of the final product C (i.e., the collapsed globules already formed), but rather of the different modes (corresponding to different scales of observation of the chain) which must collapse in a concerted way. The appropriate coordination may require a significant time to be achieved, but once it is found the final contraction step becomes increasingly fast, all the modes driving each other to equilibrium. This means that the molecules switch from the "crumpled globule" to the collapsed globule in a very short time: this all-or-none process resembles to some extent the helix–coil transition[25] which takes place in a very small temperature interval. However, a fundamental difference is to be pointed out: our description is a kinetic one, the chain collapse being followed as a function of time at a fixed temperature, whereas the helix–coil transition is usually described as a succession of equilibrium states realized through a (limited) change of temperature or of some other intensive variable of the system.

Concluding Remarks

We studied the contraction kinetics to the globular state of a stiff polymer modeled as a freely-rotating chain. The contraction proceeds in general in two distinct steps separated by a time interval (denoted as the induction time) wherein the chain size and, in particular, its free energy remain almost constant. The present results indicate that the overall process takes place in a time interval which can be significantly longer than the longest relaxation time of the unperturbed chain (see Figures 4 and 6). In fact, eq 22 implies that the total time $(\sigma t)_{final}$ to achieve the equilibrium globular state may become exceedingly large either for very long chains or in the close vicinity of the transition coordinate $(\tau B)^*$. Experimentally, the latter requirement appears to be hardly feasible: the thermal inertia of the solution suddenly cooled from the Θ temperature should lead in practice to local temperature gradients, whereas the unavoidable polydispersity of the macromolecule (unless we are dealing with a protein) would tend to blur the sharpness of the transition anyway.

We would like to point out that in the present analysis we neglected the energy barriers hindering conformational rearrangements, in agreement with what is currently done in polymer dynamics (see, e.g., refs 13–17). These barriers are at the origin of the internal viscosity displayed by polymers in high-frequency dynamical experiments,[26] in that they cause an extra energy dissipation at these short time scales forcing local chain portions to move rigidly in a concerted way.

This picture of the internal viscosity translates into an integro-differential dynamic equation.[26] Proceeding along the same lines as in ref 18, these equations would lead to very complicated kinetic equations instead of the relatively simple eq 21. However, it was shown by two of us that the internal viscosity contribution is negligible for the relatively large-scale motions[26] (for instance, the intrinsic viscosity is unaffected). On the basis of these results, it can be safely assumed that these conformational energy barriers do not affect the contraction kinetics considered here, but only the "local" rearrangements.

On the other hand, some factors were tacitly neglected in the present work, which may significantly lengthen the process. The kinetic equations, for example, ignore the friction among distant segments of the chain, which becomes more and more important during contraction and decreases the bond-rate constant σ. Chain self-knotting is also ignored, but may be likely for long chains during contraction. The knots are not permanent, at least in principle, but can slow down very effectively the contraction, in particular if they are loose. This problem should be relevant for relatively flexible chains with high molecular weights, such as the polystyrene investigated in refs 6 and 7, contributing to the large induction time reported. Conversely, more rigid and shorter chains such as a typical protein should be less prone to self-knotting, so that the time to achieve a compact structure reduces to a few seconds. From this viewpoint, therefore, our results form only a lower bound for the induction time to collapse.

Experimental results on atactic polystyrene[6,7] show that an intermediate, long lasting state is achieved upon contraction in a poor solvent, possibly corresponding to the "crumpled globule" model proposed by Grosberg and Kuznetsov.[9] Eventually, this state relaxes to a compact globule with roughly the same characteristic time as that observed to attain the intermediate state. This picture is in a remarkable agreement with that emerging from the present calculations.

Although devoid of the structural details that provide each protein molecule its specific globular structure and biochemical function, we believe the present model to be a reasonable representation of the "average" behavior of a globular protein during part of its refolding (i.e., collapse) process from the denatured state. We specifically refer to the chain shrinkage producing a quasi-collapsed state (possibly related to a sort of "molten globule"[10] lacking any local detail) missing the final, ordered structure of a globular protein. This "molten globule" has reasonably common features with our final collapsed state, whose structure is still described in terms of statistical laws in spite of its relative compactness (see also ref 27). Obviously enough, adequate experimental data are still awaited to confirm the present picture.

In this connection, we also mention the recent Monte Carlo simulation performed by Karplus *et al.*[28] on a lattice polymer wherein the repeat units have different attractive interactions to model the varying hydrophobicity of residues in a protein molecule. The basic result is that, provided there is a pronounced global minimum in the potential surface, the contraction kinetics (i.e., the protein folding) follows a relatively fast two-step process to the unique compact state. In this way, proteins having a large thermodynamic stability may also reach the native state in a relatively short time. The key feature is that after the initial contraction the molecule slowly rearranges itself by searching a strongly reduced number of possible conformations. A relatively small fraction of these conformations (estimated to about 10^6 out of 10^{18} in an 80-residue protein!) consists of possible transition states to the compact equilibrium structure; whenever one of these conformations is found, the equilibrium state is quickly reached. The search stage may be somewhat akin to what happens during the induction time, within our approach, although of course the differences between the two chain models are significant.

Acknowledgment. This work was financially supported by the "Progetto Strategico Tecnologie Chimiche Innovative", CNR, Italy, and in part by the Italian Ministry of the University and of the Scientific and Technological Research (MURST, 40%).

Appendix

1. Equation 20′ may be simplified as follows. Taking the ordered triplet $i < j < h$, we define

$$\Delta(t) = (2l^2)^{-1}[\langle r_{ih}^2(t)\rangle - \langle r_{ij}^2(t)\rangle - \langle r_{jh}^2(t)\rangle] \qquad \text{(A-1)}$$

whence we have

$$\Psi_{ijh}(t) \equiv l^{-4}\langle r_{ij}^2(t)\rangle\langle r_{jh}^2(t)\rangle - \Delta(t)^2 \qquad \text{(A-2)}$$

For the *phantom* freely-jointed chain ($g = 0$) we have $\langle r_{ih}^2\rangle = \langle r_{ij}^2\rangle + \langle r_{jh}^2\rangle$ and so $\Delta = 0$.

2. From eqs 16–20, the partial derivative of $\mathcal{A}$ in eq 21 is given by

$$\frac{\partial \mathcal{A}(t)}{\partial \alpha_p^2(t)} = \frac{3}{2}\left[1 - \frac{1}{\alpha_p^2(t)}\right] - \frac{3}{2}\tau B \sum\sum_{i<j}\left[\frac{\langle r_{ij}^2(t)\rangle}{l^2}\right]^{-5/2}\frac{\partial[\langle r_{ij}^2(t)\rangle/l^2]}{\partial \alpha_p^2(t)} - \frac{5}{2}K\sum\sum_{i<j}\left[\frac{\langle r_{ij}^2(t)\rangle}{l^2}\right]^{-7/2}\frac{\partial[\langle r_{ij}^2(t)\rangle/l^2]}{\partial \alpha_p^2(t)} - \frac{3}{2}K_1\sum\sum\sum_{i<j<h}\Psi_{ijh}(t)^{-5/2}\frac{\partial \Psi_{ijh}(t)}{\partial \alpha_p^2(t)} \qquad p = 1, 2, ..., N \qquad \text{(A-3)}$$

where from eq 14

$$\frac{\partial[\langle r_{ij}^2(t)\rangle/l^2]}{\partial \alpha_p^2(t)} = (Q_{ip} - Q_{jp})^2\mu_p^{-1} \qquad \text{(A-4)}$$

is independent of t, and from eqs 20, A-1, and A-2

$$\frac{\partial \Psi_{ijh}(t)}{\partial \alpha_p^2(t)} = [\langle r_{jh}^2(t)\rangle/l^2 + \Delta(t)]\frac{\partial[\langle r_{ij}^2(t)\rangle/l^2]}{\partial \alpha_p^2(t)} + [\langle r_{ij}^2(t)\rangle/l^2 + \Delta(t)]\frac{\partial[\langle r_{jh}^2(t)\rangle/l^2]}{\partial \alpha_p^2(t)} - \Delta(t)\frac{\partial[\langle r_{ih}^2(t)\rangle/l^2]}{\partial \alpha_p^2(t)} \qquad \text{(A-5)}$$

References and Notes

(1) Sun, T. S.; Nishio, I.; Swislow, G.; Tanaka, T. *J. Chem. Phys.* **1980**, *73*, 5971.

(2) Štepánek, P.; Koňák, C. *Collect. Czech. Chem. Commun.* **1985**, *50*, 2579.
(3) Park, I. H.; Wang, Q.-W.; Chu, B. *Macromolecules* **1987**, *20*, 1965.
(4) Allegra, G.; Ganazzoli, F. *Adv. Chem. Phys.* **1989**, *75*, 265.
(5) Kolinski, a.; Skolnik, J.; Yaris, R. *J. Chem. Phys.* **1986**, *85*, 3585.
(6) Yu, J.; Wang, Z.; Chu, B. *Macromolecules* **1992**, *25*, 1618.
(7) Chu, B.; Ying, Q.; Grosberg, A. Yu. *Macromolecules* **1995**, *28*, 180.
(8) de Gennes, P. G. *J. Phys. Lett.* **1985**, *46*, L639.
(9) Grosberg, A. Yu.; Kuznetov, D. V. *Macromolecules* **1993**, *26*, 4249.
(10) Ptitsyn, O. B. *J. Protein Chem.* **1987**, *6*, 273.
(11) Allegra, G.; De Vitis, M.; Ganazzoli, F. *Makromol. Chem., Theory Simul.* **1993**, 2, 829.
(12) Yamakawa, H. *Modern theory of polymer solutions*; Harper & Row: New York, 1971; Chapter II, Section 9c.
(13) Perico, A.; Bisio, S.; Cuniberti, C. *Macromolecules* **1984**, *17*, 2686.
(14) Zimm, B. H. *J. Chem. Phys.* **1956**, *24*, 269.
(15) Bixon, M.; Zwanzig, R. *J. Chem. Phys.* **1978**, *68*, 1896.
(16) Perico, A.; Guenza, M. *J. Chem. Phys.* **1985**, *83*, 3103.
(17) Perico, A.; Ganazzoli, F.; Allegra, G. *J. Chem. Phys.* **1987**, *87*, 3677.
(18) Allegra, G.; Ganazzoli, F. *Gazz. Chim. Ital.* **1987**, *117*, 599.
(19) Ganazzoli, F.; Fontelos, M. A. *Polymer* **1988**, *29*, 1648.
(20) Allegra, G.; Ganazzoli, F. *J. Chem. Phys.* **1985**, *83*, 397.
(21) Allegra, G.; Ganazzoli, F. *Prog. Polym. Sci.* **1991**, *16*, 463.
(22) Allegra, G.; Ganazzoli, F.; Bignotti, F.; Bolognesi, M. *Biopolymers* **1990**, *29*, 1823.
(23) Muthukumar, M. *J. Chem. Phys.* **1984**, *81*, 6272.
(24) Allegra, G.; Ganazzoli, F. *Prog. Polym. Sci.* **1991**, *16*, 463.
(25) Zimm, B. H.; Bragg, J. K. *J. Chem. Phys.* **1959**, *31*, 526.
(26) Allegra, G.; Ganazzoli, F. *Macromolecules* **1981**, *14*, 1110.
(27) Fukugita, M.; Lancaster, D.; Mitchard, M. G. *Proc. Natl. Acad. Sci. U.S.A.* **1993**, *90*, 6365.
(28) Šall, A.; Shakhnovich, E.; Karplus, M. *Nature* **1994**, *369*, 248.

MA946271+